J Ind Microbiol Biotechnol (2011) 38:1821–1835
DOI 10.1007/s10295-011-0971-2

ORIGINAL PAPER

Engineering lower inhibitor affinities in β-D-xylosidase of *Selenomonas ruminantium* by site-directed mutagenesis of Trp145

Douglas B. Jordan · Kurt Wagschal · Zhanmin Fan · Ling Yuan · Jay D. Braker · Chamroeun Heng

Received: 28 February 2011 / Accepted: 1 April 2011 / Published online: 29 April 2011

Abstract β-D-Xylosidase/α-L-arabinofuranosidase from *Selenomonas ruminantium* is the most active enzyme reported for catalyzing hydrolysis of 1,4-β-D-xylooligosaccharides to D-xylose. One property that could use improvement is its relatively high affinities for D-glucose and D-xylose ($K_i \sim 10$ mM), which would impede its performance as a catalyst in the saccharification of lignocellulosic biomass for the production of biofuels and other value-added products. Previously, we discovered that the W145G variant expresses $K_i^{\text{D-glucose}}$ and $K_i^{\text{D-xylose}}$ twofold and threefold those of the wild-type enzyme. However, in comparison to the wild type, the variant expresses 11% lower $k_{cat}^{\text{D-xylobiose}}$ and much lower stabilities to temperature and pH. Here, we performed saturation mutagenesis of W145 and discovered that the variants express K_i values that are 1.5–2.7-fold (D-glucose) and 1.9–4.6-fold (D-xylose) those of wild-type enzyme. W145F, W145L, and W145Y express good stability and, respectively, 11, 6, and 1% higher $k_{cat}^{\text{D-xylobiose}}$ than that of the wild type. At 0.1 M D-xylobiose and 0.1 M D-xylose, kinetic parameters indicate that W145F, W145L, and W145Y catalytic activities are respectively 46, 71, and 48% greater than that of the wild-type enzyme.

Keywords Glycoside hydrolase · GH43 · Saturation mutagenesis · Biofuel · Product inhibition

Abbreviations

SXA	β-D-Xylosidase/α-L-arabinofuranosidase from *Selenomonas ruminantium*
4NPX	4-nitrophenyl β-D-xylopyranoside
4NPA	4-nitrophenyl α-L-arabinofuranoside
MUX	4-methylumbelliferyl β-D-xylopyranoside
X2	D-xylobiose
SXA-C3	SXA containing these mutations W145G, T265A, P328L, and N516D

The mention of firm names or trade products does not imply that they are endorsed or recommended by the US Department of Agriculture over other firms or similar products not mentioned.

D. B. Jordan (✉) · J. D. Braker
National Center for Agricultural Utilization Research, USDA Agricultural Research Service, 1815 N. University Street, Peoria, IL 61604, USA
e-mail: douglas.jordan@ars.usda.gov

K. Wagschal · C. Heng
Western Regional Research Center, USDA Agricultural Research Service, Albany, CA 94710, USA

Z. Fan · L. Yuan
Kentucky Tobacco Research and Development Center, Department of Plant and Soil Sciences, University of Kentucky, Lexington, KY 40546, USA

Introduction

Enzymatic saccharification of lignocellulosic biomass for subsequent fermentation of the released monosaccharides to biofuels and other value-added products offers certain advantages over chemical saccharification methods largely due to the milder chemical treatment conditions that diminish production of furans and other poisons of fermenting organisms, minimize waste-stream clean up, and lower the capital cost of the reactors [10, 24, 26, 28, 29, 31]. Although enzymatic saccharification of lignocellulosic biomass can seem daunting with respect to the large number of enzyme activities needed for full deconstruction of the raw material, appropriate pretreatment of biomass

prior to enzyme addition can decrease the enzyme activities needed to about seven. For example, in addition to endoglucanase, exoglucanase and β-glucosidase needed for cellulose deconstruction, full saccharification of arabinoxylan, a major component of many biomass sources, can be achieved by employing four enzymes (two xylanases, a β-xylosidase, and an arabinofuranosidase) to completely liberate the D-xylose content [1]. Different scenarios are possible for implementation of enzymatic saccharification on the industrial scale, and a common necessity for achieving economic viability of the processes is the availability of low-cost enzymes, which encompasses factors such as high catalytic activity, inexpensive protein production, and good protein stability under reactor operating conditions.

The bifunctional β-D-xylosidase/α-L-arabinofuranosidase (EC 3.2.1.37 and EC 3.2.1.55) from *Selenomonas ruminantium* (SXA) is the most potent catalyst reported, to date, for promoting the hydrolysis of 1,4-β-D-xylooligosaccharides to D-xylose. Its k_{cat} and k_{cat}/K_m are at least tenfold greater than those reported for other β-xylosidases [16, 19, 23] when acting on oligoxylosides of increasing degrees of polymerization from xylobiose (DP2) to xylohexaose (DP6). Its strength of catalysis [16, 19, 23], good stability versus moderately low pH (stable above pH 4.0) and temperature (stable below 50°C) [15], and ease of protein production in *Escherichia coli* (30% of soluble cell protein is SXA with greater than 5 g SXA produced per liter of culture under nonoptimized conditions) [14] recommend employment of SXA in industrial processes where it would serve in the hydrolysis of herbaceous biomass (xylan fraction) to simple sugars for fermentation to fuel ethanol and other bioproducts [11, 33]. SXA belongs to glycoside hydrolase family 43 (GH43) and structural clan F of the CAZy database (Carbohydrate Active Enzymes database, http://www.cazy.org/) [4, 12]. SXA has the simplest active site possible for an efficient glycoside hydrolase by comprising only two subsites [3], subsite −1 for binding the substrate glycone and subsite +1 for binding the substrate aglycone. Because the simplicity of SXA lends itself to study, and because of the potential practical importance of SXA, a good deal has been learned about its structure–function properties [3, 16–23].

One property of SXA that clearly could use improvement is its relatively high affinity (K_i 10^{-2} M) for D-glucose and D-xylose, the two monosaccharides that would accumulate most in certain biomass saccharification reactors (e.g., corncobs). Even under conditions of simultaneous saccharification and fermentation (SSF), where the monosaccharides released from their biological polymers are immediately available for consumption by the fermenting organism, levels of D-glucose and D-xylose could adversely affect the performance of SXA. In our initial experiments to discover SXA variants with lower affinities for D-glucose and D-xylose [7], we prepared SXA variants by using error-prone PCR. In the primary screen, we selected for variants having β-xylosidase activity by using a whole-cell assay (*E. coli* containing the PCR products) with 4-methylumbelliferyl β-D-xylopyranoside (MUX, Fig. 1) as the substrate. In the secondary screen, active variants from the primary screen were assayed in cell-free reactions containing 4-nitrophenyl β-D-xylopyranoside (4NPX, Fig. 1) as substrate in the absence (A_0) and presence (A_i) of D-xylose. A single SXA variant with significantly lower activity ratio A_0/A_i than wild-type SXA was selected. Sequencing of the plasmid encoding the SXA variant (designated C3), indicated that SXA-C3 contained four mutations: W145G, T265A, P328L, and N516D (Fig. 2). Our study of the four single mutants, purified to homogeneity, determined that most of the lower affinity for

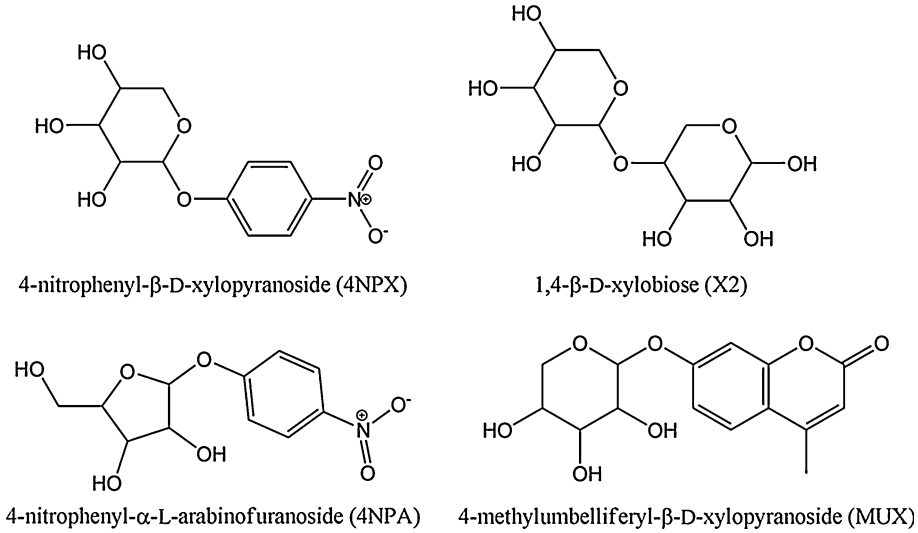

Fig. 1 Substrates of SXA discussed in the text

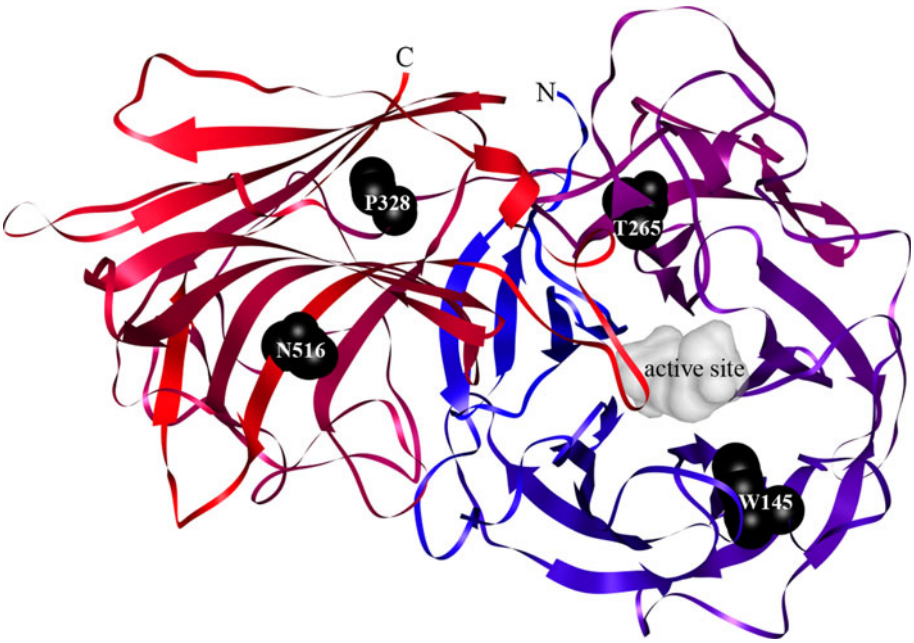

Fig. 2 Location of four mutations comprising the SXA variant, SXA-C3. A single subunit of the homotetramer is displayed. The coordinates of SXA used in producing the figure are from PDB ID 3C2U [3]

D-xylose and D-glucose is conferred by the W145G mutation, which lies 6 Å from the active site. Further experiments indicated that the W145G mutation, although remote from the active site, nevertheless influences binding of D-xylose (and by inference D-glucose) to subsite +1 and not subsite −1. The latter experiments relied on our earlier work that shows amino alcohols bind exclusively to subsite −1 and that a lower ratio $k_{cat}^{4NPX}/k_{cat}^{4NPA}$ (4NPA, 4-nitrophenyl α-L-arabinofuranoside; Fig. 1) is associated with influences on subsite −1 and a higher ratio to influences on subsite +1 [17, 21, 22]. W145G exhibits K_i values for D-glucose and D-xylose that are twofold and threefold those of wild-type SXA, respectively. Further, the k_{cat}^{4NPX} of W145G is 1.7-fold that of wild-type SXA. Importantly, however, for practical considerations, k_{cat}^{X2} (X2, D-xylobiose; Fig. 1) of W145G is 0.9-fold that of wild-type SXA and the variant's stabilities to low and high pH and high temperature are much weaker than those of wild-type SXA.

Having identified W145 as a potentially productive site for modulating monosaccharide affinities [7], for the current work we set out to perform saturation mutagenesis of W145 in hopes of finding SXA variants with properties that could improve the performance of SXA as a biomass saccharification agent. Indeed, we present here results indicating that three of the mutants (W145F, W145L, and W145Y) respectively express 11, 6, and 1% greater k_{cat}^{X2} than that of wild-type SXA, 40, 54, and 46% lower affinity for D-glucose, 48, 68, and 63% lower affinity for D-xylose, and good stabilities to variations of pH and temperature. In addition, because of the relatively large sample size involved in saturation mutagenesis, we are able to make correlations of several other properties that are also of interest.

Materials and methods

Materials and general methods

Substrates, buffers, and other reagents [7, 17, 21, 22], circular dichroism spectroscopy [17], HPLC with pulsed amperometric detection [19], isothermal calorimetry [21], SDS-PAGE analysis [15], UV-V is spectroscopy [17], and molecular modeling [7] have been described. D-Xylobiose (X2) was obtained from Wako Chemicals USA (Richmond, VA). SXA [16], SXA-C3 [7], and SXA-W145G [7] were prepared and purified to electrophoretic homogeneity as described, employing a final step of gel filtration to exchange buffer to 10 or 20 mM sodium phosphate, pH 7.0. Data were fitted to equations using the computer program Grafit (Erithacus Software) [27]. Simple weighting (constant error) was used for fitting most data. Kinetic simulations were through the computer program KinTek Explorer [13].

Construction of SXA single, double, and triple mutants

Saturation mutagenesis of the 145 site of SXA was performed by using the PCR method as described previously [32]. Plasmid pET29b-SXA(wt) [7] was amplified by the cloned Pfu DNA polymerase (Stratagene; La Jolla, CA) using primers SXA145SM-FW and SXA145SM-RV (Table 1). The amplified plasmids were evaluated by agarose gel electrophoresis and gel-purified using Wizard SV Gel and PCR Clean-up System (Promega; Madison, WI). Parental PCR template plasmid was removed from mutant library by digestion with *Dpn* I before transformation into

Table 1 PCR primers used in this study

Primer	Sequence
SXA145SM-FW	5′-CTCGTTAACATGTAC**NNK**GACCAGCGCGTATACCACC ATAAT-3′
SXA145SM-RV	5′-GTATACGCGCTGGTC**MNN**GTACATGTTAAC GAGATATTTTTTG-3′
SXA145H-FW	5′-CTCGTTAACATGTACCACGACCAGCGCGTATACCACCATAAT-3′
SXA145H-RV	5′-GTATACGCGCTGGTCGTGGTACATGTTAACGAGATATTTTTTG-3′
SXA145M-FW	5′-CTCGTTAACATGTACATGGACCAGCGCGTATACCACCATAAT-3′
SXA145M-RV	5′-GTATACGCGCTGGTCCATGTACATGTTAACGAGATATTTTTTG-3′
SXA145N-FW	5′-CTCGTTAACATGTACAACGACCAGCGCGTATACCACCATAAT-3′
SXA145N-RV	5′-GTATACGCGCTGGTCGTTGTACATGTTAACGAGATATTTTTTG-3′
SXA328L-FW	5′-GACCTTCCACAGCAGGAATGGGCACTGACATACGAAGAGCGCGATGATTT-3′
SXA328L-RV	5′-CAAAATCATCGCGCTCTTCGTATGTCAGTGCCCATTCCTGCTGTGGAAGGTC-3′
SXA516D-FW	5′-TTTCACCGGCGCATTTGTCGGCATAGATGCGATGCGATAGACATTACCGGAACGG-C3′
SXA516D-RV	5′-GCCGTTCCGGTAATGTCTATCGCATCTATGCCGACAAATGCGCCGGTGAAA-3′

Codon changes in saturation-mutagenesis primers are in *bold* font (N stands for A or C or G or T; K stands for G or T; M stands for A or C). Codon changes in single mutagenesis primers are *underlined*

E. coli BL21(DE3) cells. The SXA-145 mutants were screened by DNA sequencing. In this way, all of the SXA-145 mutants, except His, Met and Asn, were generated. The SXA-145 His, Met and Asn were generated individually in the same way by PCR with primer pairs SXA145H-FW/SXA145H-RV, SXA145M-FW/SXA145M-RV and SXA145N-FW/SXA145N-RV (Table 1). The SXA double mutant (W145G-N516D) and triple mutant (T265A-P328L-N516D) were constructed by PCR with template plasmids pET29b-SXA W145G and pET29b-SXA T265A, respectively. The primer pairs used for the construction were SXA328L-FW/SXA328L-RV and SXA516D-FW/SXA516D-RV (Table 1). The mutations were verified by DNA sequencing.

After transformation into *E. coli* BL21(DE3), cells were grown and induced as described for producing wild-type SXA [16]. All of the SXA mutant proteins prepared for this work contained C-terminal His_6-tagged appendages, which were purified to homogeneity as described [37] with the addition of a final desalting, gel filtration step into 10 mM sodium phosphate, pH 7.0. Protein concentrations of SXA and the SXA variants were determined from their absorbance at 280 nm in 10 mM sodium phosphate, pH 7.0 as calculated [9] (in units of M^{-1} cm^{-1}): wild-type SXA (129500), W145Y (125150), and all other W145 mutants (123870). Circular dichroism spectra (260–190 nm, collected for samples containing 8 μM enzyme in 10 mM sodium phosphate, pH 7.0) are similar for wild-type SXA and mutants with mean trough values [[θ]] at 214 nm (in units of 10^6 deg cm^2 $dmol^{-1}$): wild-type SXA (−3.52 ± 0.21), W145A (−2.50 ± 0.13), W145C (−2.57 ± 0.08), W145D (−2.32 ± 0.13), W145E (−2.82 ± 0.07), W145F (−2.72 ± 0.07), W145H (−2.60 ± 0.06), W145I (−2.88 ± 0.09), W145K (−2.65 ± 0.05), W145L (−2.48 ± 0.07), W145M (−2.92 ± 0.07), W145N (−2.98 ± 0.05), W145P (−2.73 ± 0.09), W145Q (−2.94 ± 0.08), W145R (−2.77 ± 0.09), W145S (−3.02 ± 0.06), W145T (−2.54 ± 0.08), W145V (−2.82 ± 0.09), W145Y (−2.98 ± 0.09), double mutant (−2.89 ± 0.10), and triple mutant (−2.84 ± 0.03).

Stokes radius determinations

Size-exclusion chromatography was used to determine the Stokes radii of the SXA-W145P variant and the wild-type SXA by using similar methods and the same chromatography column described previously [15]. Briefly, the column (2.6 × 61 cm) was packed with Toyo-Pearl 55F resin equilibrated with 10 mM sodium phosphate, 75 mM NaCl, pH 7.0 at 24−26°C with a flow rate of 1.0 ml/min. Post-column eluate was monitored continuously for absorbance at 260, 280, and 405 nm. Elution volumes (V_e) were recorded and converted to K_{av} values by using Eq. (1) where V_e is the recorded elution volume, V_0 is the void volume of the column, and V_t is the total volume of the column plus tubing connecting to the absorbance monitor. The value for V_0 was determined as 109 ml by using Blue Dextran 2000. The value of V_t was determined as 320 ml. Protein standards of known Stokes radius (R_S) and molecular weight (MW) were ferritin (R_S 61.0 Å, MW 440 kDa), catalase (R_S 52.2 Å, MW 232 kDa), and aldolase (R_S 48.1 Å, MW 158 kDa). The Stokes radii of SXA and W145P were determined from the linear regression of protein standards fitted to Eq. (2) where K_{av} is defined by Eq. 1, R_S is the Stokes radius, m is the slope and C is the constant of the standard line.

$$K_{av} = \frac{V_e - V_0}{V_t - V_0} \quad (1)$$

$$(-\mathrm{Log}K_{\mathrm{av}})^{1/2} = m^{*}R_{\mathrm{S}} + C \quad (2)$$

Enzyme-catalyzed reactions

Initial-rate reactions for determination of kinetic parameters of the SXA variants acting on 4NPX, 4NPA, and X2 were conducted as described [7]. Briefly, reactions were carried out at pH 6.0 and 25°C, and the initial rate data were fitted to Eq. (3): v is the initial velocity at the specified concentration of substrate, E_{T} is the concentration of all enzyme species in the reaction, k_{cat} is the turnover number of catalysis (expressed in moles of glycosidic bonds hydrolyzed per second per mole enzyme protomer), S is the substrate concentration, and K_{m} is the Michaelis constant. K_{i} values for D-xylose and D-glucose were determined by including three or more fixed concentrations of the inhibitors in reactions containing varied concentrations of 4NPX or 4NPA at pH 6.0 and 25°C, and the initial-rate data were fit to Eqs. (4) and (5): I is the inhibitor concentration, K_{i} is the dissociation constant for I from EI (the enzyme-inhibitor complex), and K_{is} is the dissociation constant for S from EIS (the enzyme-inhibitor-substrate complex). For the W145P mutant acting on 4NPA and X2, initial-rate data were fit to Eq. (6) (Hill equation) where n is the Hill coefficient.

$$\frac{v}{E_{\mathrm{T}}} = \frac{k_{\mathrm{cat}}S}{K_{\mathrm{m}} + S} \quad (3)$$

$$\frac{v}{E_{\mathrm{T}}} = \frac{k_{\mathrm{cat}}S}{K_{\mathrm{m}}\left(1 + \frac{I}{K_{\mathrm{i}}}\right) + S} \quad (4)$$

$$\frac{v}{E_{\mathrm{T}}} = \frac{k_{\mathrm{cat}}S}{K_{\mathrm{m}}\left(1 + \frac{I}{K_{\mathrm{i}}}\right) + S\left(1 + \frac{K_{\mathrm{m}}I}{K_{\mathrm{is}}K_{\mathrm{i}}}\right)} \quad (5)$$

$$\frac{v}{E_{\mathrm{T}}} = \frac{k_{\mathrm{cat}}S^{\mathrm{n}}}{K_{\mathrm{m}}^{\mathrm{n}} + S^{\mathrm{n}}} \quad (6)$$

Table 2 Steady-state kinetic parameters and inhibition constants for SXA and SXA variants acting on 4NPX at pH 6.0 and 25°C[a]

SXA variant	$k_{\mathrm{cat}}^{4\mathrm{NPX}}$ (s^{-1})	$k_{\mathrm{cat}}/K_{\mathrm{m}}^{4\mathrm{NPX}}$ (s^{-1} mM^{-1})	$K_{\mathrm{m}}^{4\mathrm{NPX}}$ (mM)	$K_{\mathrm{i(D\text{-}xylose)}}^{4\mathrm{NPX}}$ (mM)[c]	$K_{\mathrm{is(D\text{-}xylose)}}^{4\mathrm{NPX}}$ (mM)[c]	$K_{\mathrm{i(D\text{-}glucose)}}^{4\mathrm{NPX}}$ (mM)[a]
Wild-type[a]	27.3 ± 0.4	55.2 ± 2.2	0.494 ± 0.025	6.24 ± 0.30	16.6 ± 4.1	44.0 ± 1.9
C3[a]	50.5 ± 0.3	38.8 ± 0.4	1.30 ± 0.02	20.7 ± 0.7	38.2 ± 12.5	101 ± 2
Triple mutant[b]	26.3 ± 0.4	52.8 ± 2.1	0.498 ± 0.025	6.12 ± 0.33	17.6 ± 4.7	48.9 ± 1.8
Double mutant[c]	54.5 ± 0.2	38.8 ± 0.3	1.41 ± 0.01	19.8 ± 0.4	84.4 ± 27.0	84.0 ± 1.4
W145A	44.8 ± 0.4	41.7 ± 0.8	1.08 ± 0.03	16.2 ± 0.5	51.3 ± 15.6	65.2 ± 2.4
W145C	62.1 ± 0.4	40.6 ± 0.5	1.53 ± 0.03	21.0 ± 0.4	90.1 ± 27.0	118 ± 2
W145D	38.4 ± 0.8	34.4 ± 1.5	1.12 ± 0.07	19.3 ± 1.1	105 ± 124	88.6 ± 3.6
W145E	45.2 ± 0.3	38.3 ± 0.4	1.18 ± 0.02	16.9 ± 0.3	73.0 ± 20.1	78.5 ± 1.2
W145F	53.1 ± 0.5	54.7 ± 1.2	0.972 ± 0.029	12.0 ± 0.4	33.6 ± 7.20	72.0 ± 1.4
W145G[a]	46.9 ± 0.4	36.4 ± 0.7	1.29 ± 0.03	19.8 ± 0.6	86.5 ± 44.1	89.0 ± 1.5
W145H	63.6 ± 0.7	42.7 ± 0.9	1.49 ± 0.04	19.3 ± 0.8	39.4 ± 11.9	78.6 ± 1.6
W145I	50.4 ± 0.4	41.0 ± 0.7	1.23 ± 0.03	19.4 ± 0.5	96.2 ± 49.0	97.8 ± 1.6
W145K	53.3 ± 0.7	18.8 ± 0.3	2.84 ± 0.09	26.1 ± 0.9	65.5 ± 28.4	110 ± 2.6
W145L	58.9 ± 0.4	48.6 ± 0.8	1.21 ± 0.03	19.2 ± 0.6	37.6 ± 8.9	95.6 ± 1.5
W145M	60.3 ± 0.4	43.9 ± 0.6	1.37 ± 0.02	18.6 ± 0.5	74.4 ± 26.2	97.8 ± 1.6
W145N	38.6 ± 0.3	32.4 ± 0.5	1.19 ± 0.03	28.9 ± 1.4	10^{15}	117 ± 3
W145P	0.370 ± 0.011	0.0309 ± 0.0004	12.0 ± 0.5	ND[d]	ND	ND
W145Q	42.1 ± 0.4	31.1 ± 0.5	1.35 ± 0.3	21.8 ± 0.6	73.1 ± 27.7	112 ± 3
W145R	42.1 ± 0.3	10.8 ± 0.1	3.90 ± 0.6	28.1 ± 0.8	71.3 ± 24.5	101 ± 1
W145S	45.7 ± 0.3	33.0 ± 0.5	1.39 ± 0.03	21.4 ± 0.5	88.3 ± 37.6	102 ± 1
W145T	45.8 ± 0.3	44.5 ± 0.7	1.03 ± 0.02	18.9 ± 0.6	41.3 ± 10.6	76.2 ± 1.4
W145V	47.4 ± 0.2	40.3 ± 0.3	1.18 ± 0.01	22.0 ± 0.4	109 ± 41	103 ± 1
W145Y	71.8 ± 0.9	59.6 ± 1.6	1.20 ± 0.04	16.8 ± 0.7	39.6 ± 12.0	81.9 ± 2.4

Reactions contained 100 mM sodium succinate, ionic strength 0.3 M adjusted with NaCl, at pH 6.0 and 25°C

[a] Values from [23]

[b] Triple mutant, T265A-P328L-N516D

[c] Double mutant, W145G-N516D

[d] ND, not determined

pH and temperature stabilities

pH stabilities of SXA variants were determined as before [7]: 1 h preincubations of enzyme at varying pH (4–11) and 25°C followed by assay of enzyme acting on 5 mM 4NPX at pH 7.0. Temperature stabilities were determined in a similar fashion as before [7]: 1-h preincubations of enzyme at varying temperature (25–70°C) in 100 mM sodium succinate, 0.3 M ionic strength (adjusted with NaCl) and pH 6.0 (instead of pH 7.0 in the previous study) followed by assay of enzyme acting on 4 mM 4NPX in reactions containing 100 mM sodium succinate, 0.3 M ionic strength (adjusted with NaCl), and pH 6.0 at 25°C (instead of pH 7.0 in the previous study [7]). To determine midpoints for the pH and temperature stabilities, the enzyme activity data were fit to Eqs. (7) and (8): p is the enzyme activity after preincubation at a single pH or temperature, P is the pH-independent or temperature-independent value of the parameter (i.e., activity of enzyme not pretreated), H^+ is the proton concentration, a is an exponential term, $K_{a1}^{0.5}$ is the proton concentration where p is half of P for the first group(s) affecting P, $K_{a2}^{0.5}$ is the proton concentration where p is half of P for the second group(s) affecting P, b is an exponential term, t is the temperature, $K_t^{0.5}$ is the temperature where p is half of P, and c is an exponential term.

$$p = \frac{P}{1 + \left(\frac{H^+}{K_{a1}^{0.5}}\right)^a + \left(\frac{K_{a2}^{0.5}}{H^+}\right)^b} \quad (7)$$

$$p = \frac{P}{1 + \left(\frac{t}{K_t^{0.5}}\right)^c} \quad (8)$$

Table 3 Steady-state kinetic parameters and inhibition constants for SXA and SXA variants acting on 4NPA at pH 6.0 and 25°C

SXA variant	k_{cat}^{4NPA} (s^{-1})	k_{cat}/K_m^{4NPA} (s^{-1} mM^{-1})	K_m^{4NPA} (mM)	$K_{i(D\text{-xylose})}^{4NPA}$ (mM)
Wild type[a]	3.13 ± 0.03	4.51 ± 0.10	0.695 ± 0.019	6.52 ± 0.19
C3[a,b]	2.40 ± 0.04	3.79 ± 0.17	0.634 ± 0.036	21.8 ± 1.1
Triple mutant[c]	3.04 ± 0.02	4.20 ± 0.08	0.723 ± 0.018	6.96 ± 0.15
Double mutant[d]	2.36 ± 0.04	3.31 ± 0.14	0.715 ± 0.039	24.9 ± 0.9
W145A	2.24 ± 0.02	3.67 ± 0.11	0.612 ± 0.020	18.8 ± 0.8
W145C	2.00 ± 0.01	4.26 ± 0.07	0.468 ± 0.010	23.5 ± 0.7
W145D	2.10 ± 0.04	2.95 ± 0.09	0.713 ± 0.030	ND[e]
W145E	2.08 ± 0.01	3.51 ± 0.04	0.593 ± 0.009	20.0 ± 0.4
W145F	2.04 ± 0.02	5.14 ± 0.08	0.398 ± 0.010	ND
W145G[a]	2.14 ± 0.03	3.37 ± 0.13	0.636 ± 0.031	21.8 ± 1.1
W145H	1.45 ± 0.02	3.65 ± 0.09	0.396 ± 0.014	ND
W145I	2.48 ± 0.02	3.81 ± 0.09	0.652 ± 0.019	26.2 ± 0.9
W145K	1.48 ± 0.02	2.77 ± 0.09	0.533 ± 0.022	23.4 ± 1.0
W145L	3.15 ± 0.05	4.73 ± 0.10	0.666 ± 0.023	ND
W145M	1.77 ± 0.02	4.38 ± 0.09	0.405 ± 0.011	ND
W145N	2.54 ± 0.05	3.11 ± 0.07	0.817 ± 0.030	32.7 ± 1.7
W145P[f]				
W145Q	2.24 ± 0.02	2.84 ± 0.07	0.790 ± 0.025	26.4 ± 0.9
W145R	1.17 ± 0.01	1.34 ± 0.03	0.873 ± 0.022	30.0 ± 0.9
W145S	1.95 ± 0.01	3.06 ± 0.06	0.638 ± 0.015	25.2 ± 0.7
W145T	1.98 ± 0.02	3.76 ± 0.12	0.528 ± 0.022	21.6 ± 0.7
W145V	2.28 ± 0.02	3.41 ± 0.10	0.670 ± 0.025	27.2 ± 1.0
W145Y	1.67 ± 0.02	5.86 ± 0.14	0.285 ± 0.010	ND

Reactions contained 100 mM sodium succinate, 0.3 M ionic strength adjusted with NaCl, at pH 6.0 and 25°C

[a] Values from [23]

[b] C3, W145G-T265A-P328L-N516D

[c] Triple mutant, T265A-P328L-N516D

[d] Double mutant, W145G-N516D

[e] ND, not determined

[f] Kinetic parameters and inhibition constants were not determined due to non-Michaelis–Menten kinetics for W145P acting on 4NPA

Results and discussion

Kinetic parameters and inhibition constants were determined from the initial-rates of reactions at pH 6.0 and 25°C. The kinetic parameters, determined by fitting initial-rate data to Eq. (3) (Michaelis–Menten equation) are presented in Table 2 for enzyme acting on 4NPX, Table 3 for enzyme acting on 4NPA, and Table 4 for enzyme acting on X2. Relative kinetic parameters (4NPX/4NPA) and (X2/4NPX), comparing changes in the glycone and the aglycone, respectively, are presented in Table 5. Inhibition constants for D-glucose and D-xylose were determined for the enzyme acting on 4NPX by fitting the initial-rate data to Eqs. (4) and (5), respectively (Table 2). Equation (4) describes competitive inhibition and it determines the single inhibition constant, K_i. Equation (5) describes noncompetitive inhibition, which is needed for D-xylose because in addition to forming the enzyme-D-xylose complex that defines the K_i term, it forms the enzyme-D-xylose-4NPX complex [16, 18] that defines the K_{is} term of Eq. (5). Because the enzyme-D-xylose-4NPA complex does not form [16, 18], $K_i^{\text{D-xylose}}$ values were determined for some of the mutants acting on 4NPA with initial data fit to Eq. (4) simply to affirm that the values are similar to the $K_i^{\text{D-xylose}}$ values determined for the enzyme acting on 4NPX with the initial-rate data fitted to Eq. (5). Though statistically significant in most cases (F test evaluations), the K_{is} terms are not well determined by the experiments due to the limited solubility of 4NPX in water.

As in our initial study of SXA mutants having lower affinities than wild-type SXA for D-xylose and D-glucose [7], SXA variants of the current study, for the most part, followed Michaelis–Menten kinetics providing well-determined values for kinetic parameters and inhibition constants (except K_{is} values as mentioned) with very good reproducibility. The one exception to this, W145P of the current study, displays Michaelis–Menten kinetics when acting on 4NPX, although we were not able to study the kinetics above the K_m due to the limited water solubility of 4NPX and the high K_m (Fig. 3a). Kinetic parameters of W145P acting on 4NPX are listed in Table 2. However, when acting on substrate 4NPA at pH 6.0, the saturation curve of W145P (1.8 μM protomer) displays positive cooperativity of 4NPA binding and could not be saturated with the substrate, the latter due to the limited water solubility of 4NPA (Fig. 3b). A Hill coefficient of 1.8 was determined by fitting the initial-rate data to Eq. (6). Also, when acting on substrate X2, the saturation curve shows positive cooperativity of binding (Fig. 3c). A Hill coefficient of 2.5 was determined. Because of the apparent binding cooperativity of W145P acting on 4NPA and X2 (Hill coefficient near 2), we considered the possibility that the enzyme's quaternary structure was undergoing change upon contacting substrate. The native SXA is a homotetramer and the tetramer to dimer dissociation constant is 7 nM at pH 7.0 [3]. Therefore, it seemed possible that W145P in its dimeric state was converted to a more active tetrameric state upon binding 4NPA. The hypothesis was tested by determining the Stokes radius of W145P at a similar protomer concentration (23 μM protomer at elution peak) as that used in hydrolysis reactions and compared it to that of the native SXA (12 μM protomer at elution peak). Size-exclusion chromatography of the two proteins (Fig. 3d) determined Stokes radii of 54.8 ± 0.8 Å

Table 4 Steady-state kinetic parameters for SXA and SXA variants acting on X2 at pH 6.0 and 25°C

SXA variant	k_{cat}^{X2} (s^{-1})	k_{cat}/K_m^{X2} (s^{-1} mM^{-1})	K_m^{X2}(mM)
Wild type[a]	175 ± 3	116 ± 7	1.51 ± 0.09
C3[b,c]	204 ± 6	32.8 ± 1.4	6.21 ± 0.41
Triple mutant[d]	139 ± 6	113 ± 12	1.24 ± 0.17
Double mutant[e]	136 ± 2.3	36.0 ± 1.5	3.79 ± 0.21
W145A	149 ± 5	42.2 ± 3.9	3.52 ± 0.42
W145C	129 ± 5	44.0 ± 4.9	3.52 ± 0.42
W145D	184 ± 3	35.4 ± 0.5	5.21 ± 0.14
W145E	146 ± 4	40.5 ± 2.7	3.61 ± 0.31
W145F	192 ± 7	63.0 ± 2.7	3.05 ± 0.21
W145G[b]	155 ± 2	34.5 ± 1.1	4.48 ± 0.20
W145H	167 ± 7	26.2 ± 0.9	6.36 ± 0.43
W145I	166 ± 3	45.5 ± 2.0	3.64 ± 0.20
W145K	121 ± 8	22.2 ± 3.0	5.42 ± 1.00
W145L[a]	185 ± 4	55.1 ± 3.2	3.36 ± 0.12
W145M	177 ± 9	30.1 ± 1.3	5.88 ± 0.50
W145N	174 ± 6.1	25.8 ± 0.7	6.74 ± 0.38
W145P[f]			
W145Q	145 ± 4	41.1 ± 2.9	3.53 ± 0.33
W145R	123 ± 3	17.3 ± 0.7	7.13 ± 0.42
W145S	147 ± 5	42.0 ± 3.4	3.50 ± 0.37
W145T	152 ± 7	43.8 ± 5.3	3.46 ± 0.55
W145V	165 ± 3	46.0 ± 2.1	3.58 ± 0.21
W145Y	178 ± 3.4	45.2 ± 0.9	3.94 ± 0.14

Reactions contained 100 mM sodium succinate, ionic strength 0.3 M adjusted with NaCl, at pH 6.0 and 25°C

[a] Values determined in triplicate. Means and standard deviations are indicated

[b] Values from [23]

[c] C3, W145G-T265A-P328L-N516D

[d] Triple mutant, T265A-P328L-N516D

[e] Double mutant, W145G-N516D

[f] Kinetic parameters and inhibition constants were not determined due to non-Michaelis–Menten kinetics for W145P acting on X2

(W145P) and 56.0 ± 0.8 Å (wild-type SXA), expected values for the SXA tetramer [15], thus rejecting the hypothesis that a perturbed quaternary structure provides an explanation for the cooperative binding kinetics of W145P.

Affinities for D-xylose and D-glucose expressed by SXA variants

Of the four mutations present in SXA-C3 ($K_i^{D\text{-xylose}}$ 20.7 mM, Table 2), W145G ($K_i^{D\text{-xylose}}$ 19.8 mM, Table 2) accounts for most of the loss in affinity for D-xylose relative to wild-type SXA ($K_i^{D\text{-xylose}}$ 6.24 mM, Table 2). Whereas two mutations T265A ($K_i^{D\text{-xylose}}$ 6.33 mM) and P328L ($K_i^{D\text{-xylose}}$ 6.57 mM) have D-xylose affinities similar to wild-type SXA, the fourth mutation N516D ($K_i^{D\text{-xylose}}$ 8.06 mM) clearly has lower affinity [7]. To follow up on these determinations, we prepared the triple mutant (T265A-P328L-N516D) for the current work to inquire whether the lowered affinities for D-xylose and D-glucose are provided by SXA-C3 (W145G, T265A, P328L, and N516D) without the contribution of W145G. The determinations indicate that the triple mutant ($K_i^{D\text{-xylose}}$ 6.12 mM, Table 2) has similar affinity for D-xylose as wild-type SXA ($K_i^{D\text{-xylose}}$ 6.24 mM, Table 2). As well, the two proteins have similar affinities for D-glucose (Table 2). Therefore, the lowered affinities for D-xylose and D-glucose provided by the single mutant N516D are masked in the triple mutant and likely in SXA-C3. Also, as a follow up on the potential utility of the N516D mutation, we prepared the double mutant (W145G-N516D) to inquire whether the lowered affinities of the individual mutations were additive. The double mutant ($K_i^{D\text{-xylose}}$ 19.8 mM, Table 2) has equal affinity for D-xylose as the single mutant W145G ($K_i^{D\text{-xylose}}$ 19.8 mM, Table 2) indicating that the mutations are not additive and that there is no advantage to this parameter in their combination over W145G alone.

The bulk of the determined inhibition constants presented here derive from saturation mutagenesis of SXA site 145. Substitution of W145 with any other amino acid results in

Table 5 Relative steady-state kinetic parameters for SXA and SXA variants acting on 4NPX, 4NPA, and X2 at pH 6.0 and 25°C

SXA variant	$k_{cat}^{4NPX/4NPA}$	$k_{cat}^{X2/4NPX}$	$k_{cat}/K_m^{4NPX/4NPA}$	$k_{cat}/K_m^{X2/4NPX}$	$K_m^{4NPX/4NPA}$	$K_m^{X2/4NPX}$
Wild type	8.71 ± 0.14	6.41 ± 0.14	12.3 ± 0.6	2.10 ± 0.15	0.711 ± 0.041	3.07 ± 0.16
C3[a]	21.0 ± 0.4	4.03 ± 0.12	10.2 ± 0.5	0.846 ± 0.036	2.05 ± 0.12	4.77 ± 0.32
Triple mutant[b]	8.65 ± 0.14	5.31 ± 0.22	12.6 ± 0.6	2.13 ± 0.25	0.689 ± 0.039	2.49 ± 0.37
Double mutant[c]	23.1 ± 0.4	2.50 ± 0.04	11.7 ± 0.5	0.928 ± 0.040	1.97 ± 0.11	2.70 ± 0.15
W145A	20.0 ± 0.3	3.31 ± 0.12	11.4 ± 0.4	1.01 ± 0.10	1.76 ± 0.08	3.27 ± 0.40
W145C	31.1 ± 0.3	2.08 ± 0.08	9.54 ± 0.20	1.08 ± 0.12	3.26 ± 0.09	1.92 ± 0.27
W145D	18.3 ± 0.5	4.80 ± 0.13	11.7 ± 0.6	1.03 ± 0.05	1.57 ± 0.12	4.67 ± 0.31
W145E	21.7 ± 0.2	3.23 ± 0.09	10.9 ± 0.2	1.06 ± 0.07	1.99 ± 0.04	3.06 ± 0.27
W145F	26.0 ± 0.4	3.62 ± 0.13	10.6 ± 0.3	1.15 ± 0.06	2.44 ± 0.09	3.14 ± 0.24
W145G	21.9 ± 0.4	3.30 ± 0.06	10.8 ± 0.5	0.947 ± 0.035	2.03 ± 0.11	3.48 ± 0.18
W145H	44.0 ± 0.8	2.62 ± 0.11	11.7 ± 0.4	0.613 ± 0.024	3.76 ± 0.17	4.27 ± 0.31
W145I	20.3 ± 0.2	3.28 ± 0.06	10.8 ± 0.3	1.11 ± 0.05	1.89 ± 0.07	2.96 ± 0.18
W145K	36.1 ± 0.6	2.27 ± 0.14	6.77 ± 0.25	1.19 ± 0.16	5.33 ± 0.27	1.91 ± 0.36
W145L	18.7 ± 0.3	3.14 ± 0.07	10.3 ± 0.3	1.13 ± 0.07	1.82 ± 0.07	2.77 ± 0.12
W145M	34.1 ± 0.4	2.94 ± 0.15	10.0 ± 0.2	0.686 ± 0.031	3.39 ± 0.11	4.28 ± 0.37
W145N	15.2 ± 0.3	4.51 ± 0.16	10.4 ± 0.3	0.797 ± 0.025	1.46 ± 0.07	5.66 ± 0.34
W145P[d]						
W145Q	18.8 ± 0.2	3.44 ± 0.10	11.0 ± 0.3	1.32 ± 0.10	1.71 ± 0.07	2.61 ± 0.25
W145R	36.0 ± 0.4	2.93 ± 0.07	8.05 ± 0.17	1.60 ± 0.07	4.47 ± 0.13	1.83 ± 0.11
W145S	23.4 ± 0.2	3.21 ± 0.10	10.8 ± 0.3	1.27 ± 0.10	2.17 ± 0.07	2.52 ± 0.27
W145T	23.1 ± 0.3	3.31 ± 0.16	11.8 ± 0.4	0.985 ± 0.121	1.95 ± 0.09	3.36 ± 0.54
W145V	20.8 ± 0.2	3.48 ± 0.06	11.8 ± 0.4	1.14 ± 0.05	1.75 ± 0.07	3.05 ± 0.18
W145Y	43.0 ± 0.8	2.48 ± 0.06	10.2 ± 0.4	0.758 ± 0.025	4.23 ± 0.21	3.27 ± 0.17

Ratios of individual kinetic parameters that are listed in Tables 2–4

[a] C3, W145G-T265A-P328L-N516D

[b] Triple mutant, T265A-P328L-N516D

[c] Double mutant, W145G-N516D

[d] Kinetic parameters were not determined for W145P acting on 4NPA and X2 due to non-Michaelis–Menten kinetics

lowered affinity for D-xylose and D-glucose (Table 2; Fig. 4a, b). $K_i^{D\text{-xylose}}$ values of the site 145 replacements vary from 12.0 mM (W145F) to 28.9 mM (W145 N) or factors of 1.9–4.6 that of the wild-type value. Both positively charged amino acid side chains are good at lowering affinity for D-xylose: W145K ($K_i^{D\text{-xylose}}$ 26.1 mM) and W145R ($K_i^{D\text{-xylose}}$ 28.1 mM). In the case of glucose, $K_i^{D\text{-glucose}}$ values of the site 145 replacements vary from 65.2 mM (W145A) to 117 mM (W145 N) or factors of 1.5–2.7 that of the wild-type value. Similar to $K_i^{D\text{-xylose}}$, W145 N ($K_i^{D\text{-glucose}}$ 117 mM) expresses the lowest affinity for D-glucose and W145K ($K_i^{D\text{-glucose}}$ 110 mM) and W145R ($K_i^{D\text{-glucose}}$ 101 mM) are among the lowest in affinity for D-glucose. The structural similarities of D-glucose and D-xylose and the similarities of their binding modes to SXA are reflected in the plot of $K_i^{D\text{-glucose}}$ versus $K_i^{D\text{-xylose}}$ for mutants containing single-site changes at position 145 (Fig. 4a). While important for SXA stability (vide infra), hydrophobicity of the amino acid side chain, using the empirically determined hydrophobicity scale [8] as modified [38], does not correlate well with $K_i^{D\text{-xylose}}$ or $K_i^{D\text{-glucose}}$ (Fig. 4b).

Kinetic parameters of SXA variants acting on 4NPX, 4NPA, and X2

For mutants containing a single-site mutation at position 145, kinetic parameters are plotted versus $K_i^{D\text{-xylose}}$ in Fig. 5a (4NPX), Fig. 5b (4NPA), and Fig. 5c (X2). The

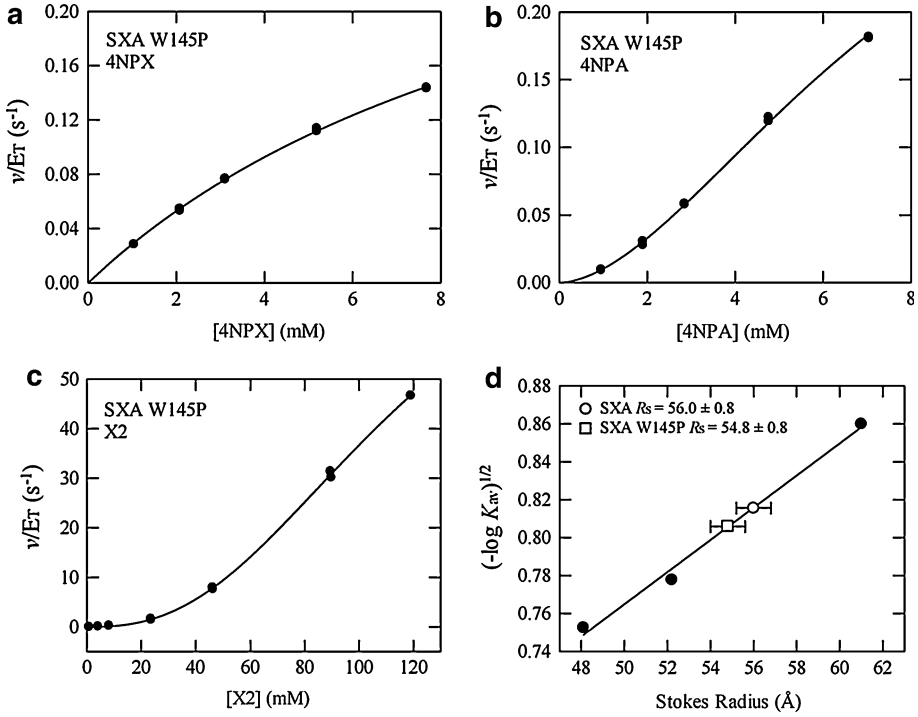

Fig. 3 Kinetic and quaternary structure properties of the SXA variant, W145P. **a** W145P acting on 4NPX. Initial rate data were fit to Eq. (3) (Michaelis–Menten equation) to produce the curve. Kinetic parameters are listed in Table 2. **b** W145P acting on 4NPA. Initial-rate data points were fit to Eq. (6) (Hill equation) to produce the curve: $k_{cat}^{4NPA} = 0.413 \pm 0.054\ s^{-1}$, $K_m^{4NPA} = 7.99 \pm 0.96$ mM, n (Hill coefficient) $= 1.77 \pm 0.05$. **c** W145P acting on X2. Initial-rate data points were fit to Eq. (6) to produce the curve: $k_{cat}^{X2} = 91.5 \pm 6.0\ s^{-1}$, $K_m^{X2} = 117 \pm 6$ mM, n (Hill coefficient) $= 2.55 \pm 0.08$. **d** Determination of Stokes radii of W145P and wild-type SXA by using size-exclusion chromatography

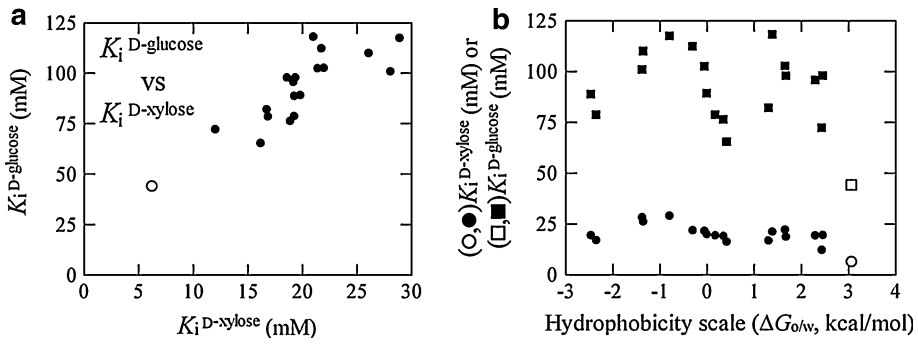

Fig. 4 Relationships between K_i values for D-xylose and D-glucose and hydrophobicity of amino acid side chains. **a** Plot of $K_i^{D\text{-glucose}}$ versus $K_i^{D\text{-xylose}}$ for wild-type SXA (*hollow circles*) and mutations of SXA at site 145 (*filled circles*). K_i values are listed in Table 2. **b** Plot of $K_i^{D\text{-glucose}}$ and $K_i^{D\text{-xylose}}$ versus hydrophobicity of the amino acid side-chain occupying site 145. Wild-type SXA (*hollow symbols*) and mutations of SXA at site 145 (*filled symbols*). The hydrophobicity scale [8] has been modified as described [38]

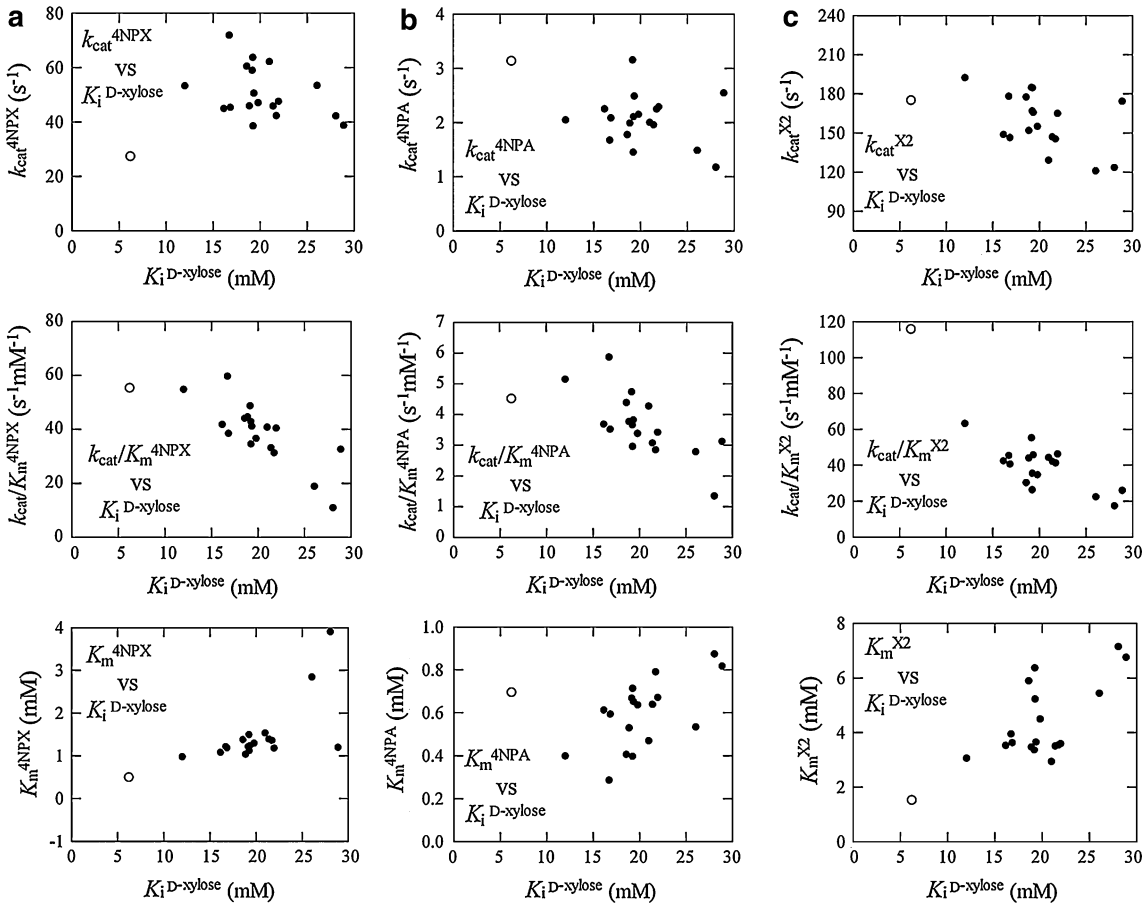

Fig. 5 Kinetic parameters versus $K_i^{D\text{-xylose}}$ for wild-type SXA and mutations of SXA at site 145. Wild-type coordinates are indicated by the *hollow circle*; mutant coordinates are indicated by the *filled circles*. Kinetic parameters are listed in Table 2 (4NPX), Table 3 (4NPA), and Table 4 (X2). $K_i^{D\text{-xylose}}$ values are listed in Table 2

graphics provide a convenient means for comparing parameter values and demonstrate, for the most part, that the values of the wild-type SXA stand apart from the site 145 mutants.

Increased k_{cat}^{4NPX} and K_m^{4NPX} and lowered k_{cat}/K_m^{4NPX} of SXA-C3 and SXA-W145G mutants relative to those of wild-type SXA [7], are also seen in most of the mutants prepared for this study (Table 2; Fig. 5a). An exception is the triple mutant (T265A-P328L-N516D), which has similar kinetic parameters for acting on 4NPX as wild-type SXA. The highest k_{cat}^{4NPX} is provided by the W145Y mutation (k_{cat}^{4NPX} 71.8 s^{-1}), which is 2.6-fold that of wild-type SXA (k_{cat}^{4NPX} 27.3 s^{-1}). W145Y is also exceptional in that it is the only mutant, single or otherwise, that has a higher k_{cat}/K_m^{4NPX} than wild-type SXA (59.6 $s^{-1}mM^{-1}$vs. 55.2 $s^{-1}mM^{-1}$). Had these parameters been for the enzyme acting on X2 or xylooligosaccharides, then W145Y would offer substantial improvements in performance under most reaction conditions that would be encountered in reactors for saccharification of biomass. Combined with its threefold lower affinity for D-xylose and twofold lower affinity for D-glucose than wild-type enzyme, W145Y is far better at promoting hydrolysis of 4NPX to completion than wild-type SXA.

Lower k_{cat}^{4NPA} and k_{cat}/K_m^{4NPA} of the SXA-C3 mutant and SXA-W145G in comparison to wild-type SXA [7] are also expressed by most of the mutants of this study (Table 3). The two exceptions, W145F and W145Y, have higher k_{cat}/K_m^{4NPA}, due entirely to lower K_m^{4NPA} values as their k_{cat}^{4NPA} values are considerably lower than wild-type SXA (Table 3; Fig. 5b).

In terms of practical importance, of course, performance of the enzyme acting on X2 is the key indicator provided in this study. Interestingly, k_{cat}^{X2} of the C3 mutant is 1.17-fold that of wild-type SXA (Table 4). However, the double mutant (k_{cat}^{X2} 136 s^{-1}), triple mutant (k_{cat}^{X2} 139 s^{-1}), and single mutant (W145G, k_{cat}^{X2} 155 s^{-1}) all display k_{cat}^{X2} values that are substantially lower than that of wild-type SXA (k_{cat}^{X2} 175 s^{-1}), indicating that SXA-C3 (k_{cat}^{X2} 204 s^{-1}) displays beneficial k_{cat}^{X2} synergism when the triple mutant

(k_{cat}^{X2} 139 s^{-1}) and W145G (k_{cat}^{X2} 155 s^{-1}) mutations are combined.

On average, the single-site mutants display 9% lower k_{cat}^{X2} values than wild-type SXA and 66% lower k_{cat}/K_m^{X2} values, the latter due mainly to their larger K_m^{X2} values, which are twofold to fivefold that of the wild type (Table 4; Fig. 5c). W145L (k_{cat}^{X2} 185 s^{-1}) and W145F (k_{cat}^{X2} 192 s^{-1}) display the highest k_{cat}^{X2} values, 1.06-fold and 1.10-fold that of the wild type, though the corresponding k_{cat}/K_m^{X2} values are 0.48-fold and 0.54-fold that of wild-type SXA. As presented below, W145Y is the most stable of the W145 mutants to challenges of pH and temperature. W145Y expresses modestly higher k_{cat}^{X2} 178 s^{-1} than that of the wild-type SXA (k_{cat}^{X2} 175 s^{-1}). The higher k_{cat}^{X2}, $K_i^{D\text{-xylose}}$, $K_i^{D\text{-glucose}}$, and K_m^{X2} values combine to favor the performance of W145F, W145L, and W145Y over that of wild-type SXA under high concentrations of X2 and inhibitors expected in biomass saccharification reactors. For example, if v/E_T values are calculated by substituting the kinetic parameters of wild-type SXA, W145F, W145L, and W145Y into Eq. (5) with D-xylose set at 100 mM and X2 set at 100 mM, then v/E_T values of W145F, W145L, and

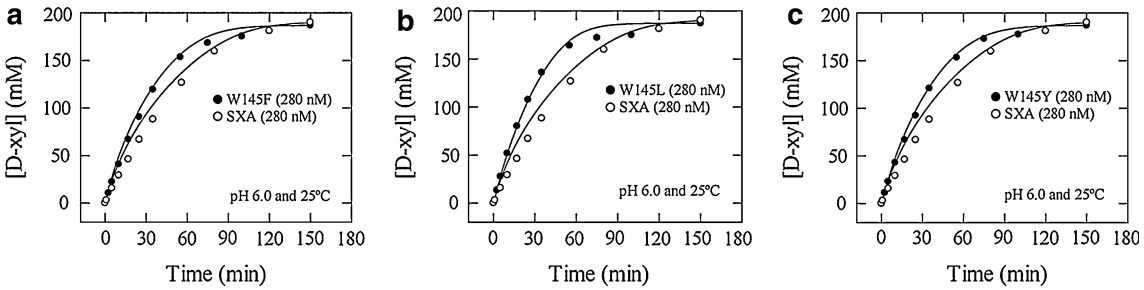

Fig. 6 Comparisons of progress curves of W145F, W145L, and W145Y (acting on 93.5 mM X2) with wild-type SXA (acting on 95.1 mM X2) at pH 6.0 and 25°C. Reactions contained 280 nM enzyme active sites, 93.5 mM or 95.1 mM X2, 100 mM sodium succinate (ionic strength 0.3 M, adjusted with NaCl), pH 6.0 and 25°C. Reactions were initiated by the addition of 280 nM enzyme active sites (final concentration). Aliquots were removed at the time intervals indicated, mixed with buffer to raise pH to above 10.4, and analyzed for D-xylose by HPLC with pulsed amperometric detection as described [19]. Observed concentrations of D-xylose are plotted (*hollow circles* for wild-type SXA and *filled circles* for W145 mutants). *Curves* are drawn by substituting kinetic parameters of Eq. (5) from Tables 2 and 4 and X2 concentrations into the computer program KinTek Explorer [13] for simulating reaction progressions. **a** W145F and wild-type SXA. **b** W145L and wild-type SXA. **c** W145Y and wild-type SXA

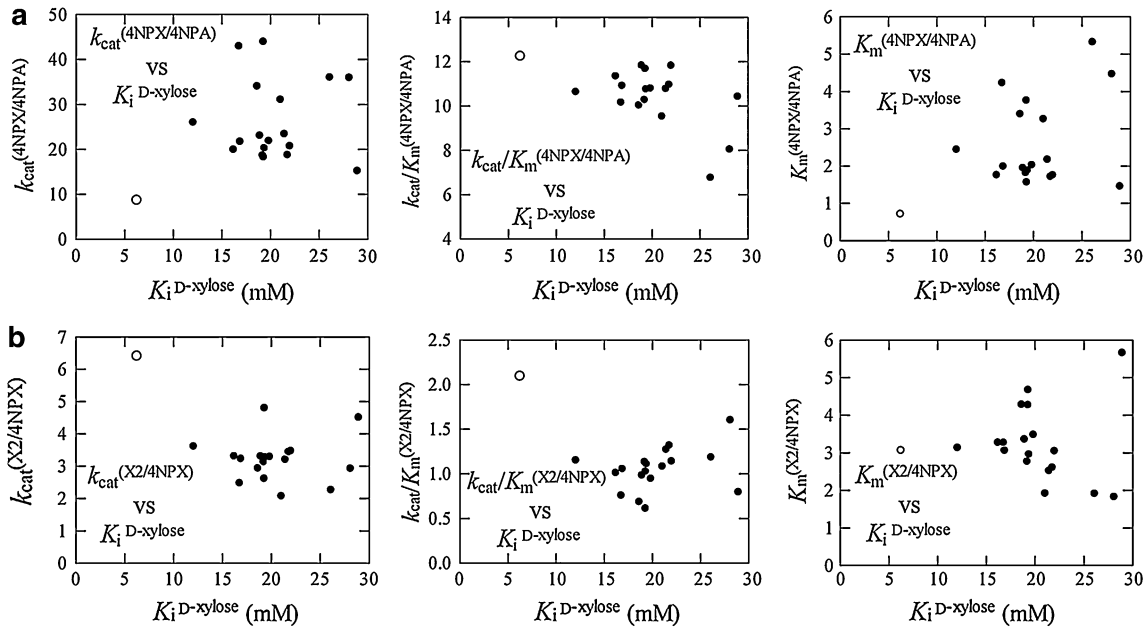

Fig. 7 Relative kinetic parameters versus $K_i^{D\text{-xylose}}$ for mutations of SXA at site 145. Wild-type values are indicated by the *hollow circles*; mutant values are indicated by the *filled circles*. Relative kinetic parameters are listed in Table 5. $K_i^{D\text{-xylose}}$ values are listed in Table 2. **a** Relative kinetic parameters (4NPX/4NPA). **b** Relative kinetic parameters (X2/4NPX)

W145Y are 1.46-fold, 1.71-fold, and 1.48-fold, respectively, of that of the wild-type SXA. This is further demonstrated by inspection of the reaction progress curves of Fig. 6, where the W145 mutants (280 nM active sites acting on 93.5 mM X2) are more effective than the wild-type SXA (280 nM active sites acting on 95.1 mM X2) at catalyzing conversion of X2 to D-xylose at pH 6.0 and 25°C; times for conversion of half of the X2 to D-xylose are 31 min (wild type), 23 min (W145F), 21 min (W145L), and 24 min (W145Y); times for 90% conversion of X2 to D-xylose are 88 min (wild type), 66 min (W145F), 55 min (W145L), and 65 min (W145Y).

Relative kinetic parameters

Relative kinetic parameters for 4NPX/4NPA and for X2/4NPX, comparing differences in the glycone and aglycone of substrate, respectively, are presented in Table 5. For the single-site mutants of position 145, the ratios are plotted versus $K_i^{\text{D-xylose}}$ in Fig. 7a (4NPX/4NPA) and Fig. 7b (X2/4NPX). As seen, $k_{cat}^{4NPX/4NPA}$ values of all variants with mutation at position 145 are greater than that of the wild-type SXA, with $k_{cat}^{4NPX/4NPA}$ values of site-specific mutants at position 145 1.7-fold to 5.1-fold that of wild-type SXA. Because energy barriers for interconversion of furanose conformations are 7 kcal/mol lower than those of pyranoses [6] and the recognized importance of the energy barrier of conformational inversion of pyranoses to hydrolysis of pyranosides [2, 5, 25, 30, 34–36], mutations of SXA effecting lower 4NPX/4NPA ratios of k_{cat} values than that of wild-type SXA identify wild-type residues involved in promoting substrate distortion (D-xylopyranosyl moiety) to its reactive conformation [17]. Active-site mutations expressing $k_{cat}^{4NPX/4NPA}$ values lower than wild-type SXA have been located in subsite −1 surrounding the glycone, while mutations effecting $k_{cat}^{4NPX/4NPA}$ values higher than that of the wild type are located in subsite +1 surrounding the aglycone. Mutations that produce higher $k_{cat}^{4NPX/4NPA}$ ratios than that of wild-type SXA, such as reported here for position 145 variants, identify native residues as promoting other events of the single transition-state reaction mechanism conducted by SXA such as protonation of the aglycone leaving group or C1 migration [22]. The $k_{cat}^{4NPX/4NPA}$ ratio of W145G is 2.5-fold that of wild-type SXA and was supporting evidence in conjunction with subsite-specific inhibitor binding studies for previous assignment of the residue's influence on $K_i^{\text{D-xylose}}$ and $K_i^{\text{D-glucose}}$ as through subsite +1 [7], with the present $k_{cat}^{4NPX/4NPA}$ results further substantiating the conclusion that the position 145 mutations influence subsite +1 in changing catalytic events.

Because X2 contains the energetically more difficult xylosyl glycone in common with 4NPX and X2, which obviously facilitates SXA-catalyzed hydrolysis of X2 (xylosyl aglycone) over 4NPX (4-nitrophenol aglycone) for wild-type SXA as the $k_{cat}^{X2/4NPX}$ value is 6.4 for wild type, it might be expected that mutations that lower $k_{cat}^{X2/4NPX}$ are associated with facilitating protonation of the aglycone leaving group, as found for the E186A mutant [22], or C1 migration events. Indeed the W145G mutant expresses $k_{cat}^{X2/4NPX}$ 3.30, half that of the wild-type SXA, suggesting that the mutation impacts subsite +1 of SXA. Affirming this designation, all of the site 145 mutations express lower $k_{cat}^{X2/4NPX}$ values than that of wild-type SXA (Table 5; Fig. 7b). Another indication that W145G affects events at subsite +1 is that it expresses higher K_{is} values than that of wild-type SXA (Table 2, [7]). K_{is} is

Table 6 Temperature and pH stabilities of wild-type SXA and SXA variants

SXA variant	$K_t^{0.5}$ (°C)	p$K_{a1}^{0.5}$	p$K_{a2}^{0.5}$
Wild-type[a]	60.0 ± 0.3	4.12 ± 0.01	11.4 ± 1.0
C3	34.7 ± 0.1	5.54 ± 0.01[b]	8.02 ± 0.01[b]
Triple mutant[b]	60.6 ± 0.3	4.23 ± 0.01	12.2 ± 0.17
Double mutant[c]	31.1 ± 0.2	5.89 ± 0.01	7.82 ± 0.01
W145A	44.4 ± 0.1	5.51 ± 0.01	7.96 ± 0.09
W145C	48.5 ± 0.2	5.03 ± 0.01	9.71 ± 0.01
W145D	36.0 ± 0.6	5.23 ± 0.01	7.57 ± 0.01
W145E	42.8 ± 0.1	5.04 ± 0.01	8.17 ± 0.01
W145F	54.7 ± 0.3	4.55 ± 0.02	9.97 ± 0.73
W145G[a]	33.7 ± 0.3	5.58 ± 0.11	7.92 ± 0.06
W145H	52.5 ± 0.2	4.98 ± 0.01	9.99 ± 0.05
W145I	43.7 ± 0.1	5.02 ± 0.14	9.32 ± 0.01
W145K	30.3 ± 0.1	5.55 ± 0.01	7.78 ± 0.10
W145L	47.1 ± 0.1	4.93 ± 0.67	9.84 ± 0.04
W145M	49.0 ± 02	4.93 ± 0.62	9.96 ± 0.12
W145N	47.7 ± 0.2	4.93 ± 0.38	9.94 ± 0.10
W145P	43.0 ± 0.8	5.24 ± 0.01	8.32 ± 0.01
W145Q	47.9 ± 0.2	5.02 ± 0.01	9.84 ± 0.02
W145R	37.0 ± 0.3	5.43 ± 0.42	7.67 ± 0.28
W145S	45.6 ± 0.3	5.03 ± 0.01	9.35 ± 0.01
W145T	44.9 ± 0.3	4.95 ± 0.30	9.46 ± 0.01
W145V	46.3 ± 0.6	5.02 ± 0.01	9.83 ± 0.02
W145Y	55.1 ± 0.2	4.53 ± 0.05	10.03 ± 0.35

For temperature stability, enzyme was preincubated for 1 h at varied temperatures and pH 6.0. Aliquots of enzyme were assayed for remaining catalytic activity with 4NPX at pH 6.0 and 25°C. The remaining activity data were fit to Eq. (8) to determine half-activity temperature ($K_t^{0.5}$). For pH stability, enzyme was preincubated 1 h at varied pH and 25°C and assayed for remaining activity with 4NPX at pH 7.0 and 25°C. The remaining activity was fit to Eq. (7) to determine half-activity pH on the acidic side ($K_{a1}^{0.5}$) and basic side ($K_{a2}^{0.5}$)

[a] Values from [23]

[b] Triple mutant, T265A-P328L-N516D

[c] Double mutant, W145G-N516D

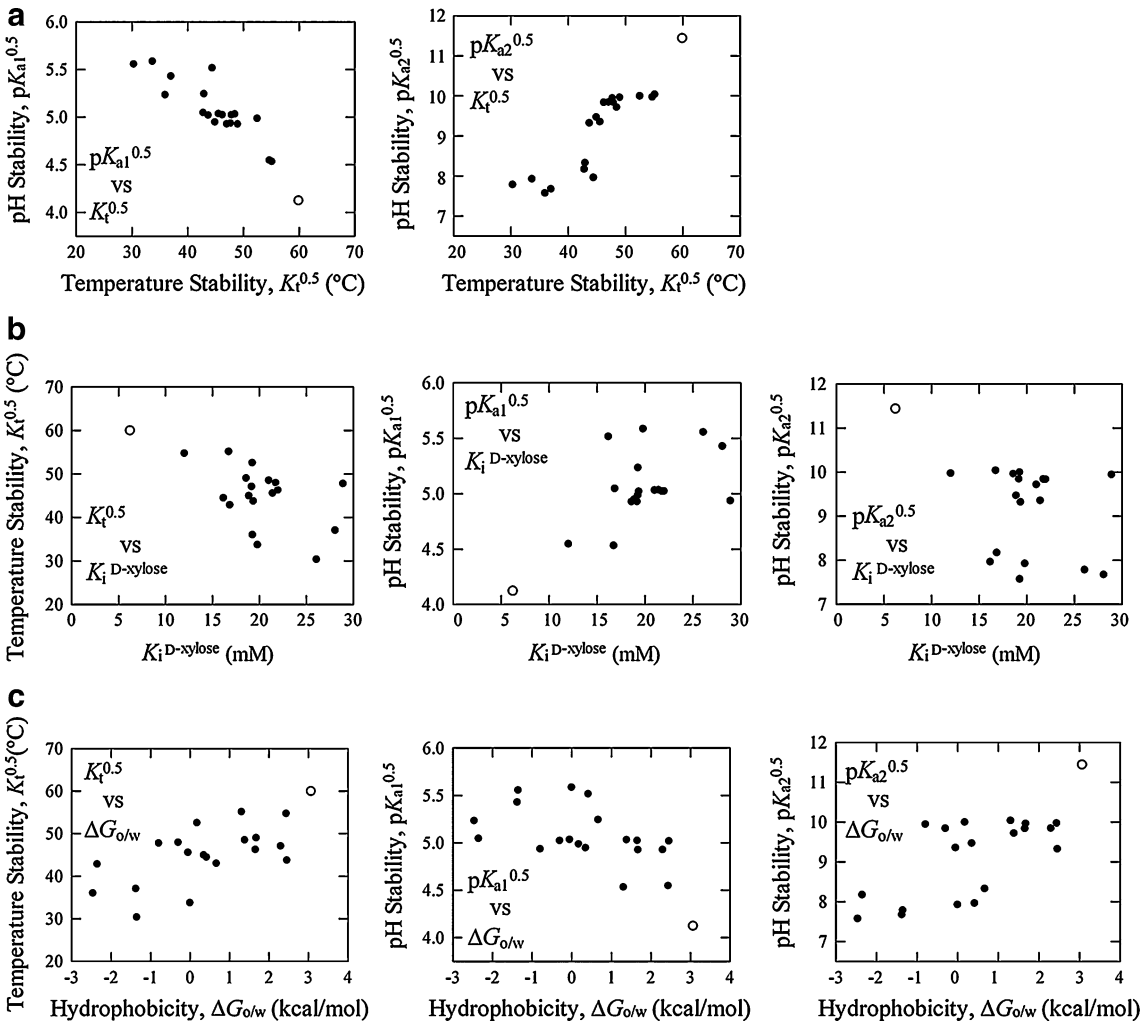

Fig. 8 Temperature and pH stabilities of wild-type SXA and site-directed mutants of SXA at position 145. Temperature stabilities and pH stabilities are listed in Table 6. Wild-type SXA (*hollow circles*) and mutants (*filled circles*). **a** pH stabilities versus temperature stabilities. Acidic side, $pK_{a1}^{0.5}$. Basic side, $pK_{a2}^{0.5}$. **b** Temperature stabilities and pH stabilities versus $K_i^{D\text{-xylose}}$. **c** pH stabilities and temperature stabilities versus hydrophobicity of amino acid side chain

the dissociation constant of 4NPX from the enzyme-D-xylose-4NPX ternary complex, in which the xylosyl moiety of 4NPX is thought to bind to subsite +1 and D-xylose in subsite −1 [18]. All of the mutations at position 145 cause loss of affinity at subsite +1 for 4NPX as indicated by the increased K_{is} values of Table 2. Therefore, both relative kinetic parameters and K_{is} trend results are consistent with binding and catalytic events being modulated by mutations at position 145 through changes in subsite +1.

pH and temperature stabilities

Stabilities of the mutants to high temperature were determined from preincubations of enzyme for 1 h at varied temperatures and pH 6.0 followed by catalytic activity assays at pH 6.0 and 25°C of preincubated enzyme acting on 4NPX. Stabilities to low pH and high pH were determined from preincubations of enzyme for 1 h at varied pH and 25°C followed by catalytic activity assays at pH 7.0 and 25°C of preincubated enzyme acting on 4NPX. Stability is expressed as the temperature (high temperature, $K_t^{0.5}$) or pH (low pH, $K_{a1}^{0.5}$; high pH, $K_{a2}^{0.5}$) at which half of the catalytic activity remains after the 1-h preincubation (Table 6).

Interestingly, Trp is the most hydrophobic amino acid based on solvation free energy [38], and all of the single-site mutations of W145 confer lower temperature and pH stabilities. Among the position 145 mutants, temperature stability correlates well with pH stability on the acidic side and the basic side (Fig. 8a). In addition, while temperature and pH stabilities correlate with $K_i^{D\text{-xylose}}$, there is enough variation to provide some mutants with both lowered affinities for D-xylose (and D-glucose) and good stabilities

to temperature and pH extremes (Fig. 8b). Finally, the pH and temperature stabilities correlate fairly well with hydrophobicity of the substituted amino acid side chain at position 145 (Fig. 8c).

Conclusions

This work follows-up on our initial study [7] that revealed position 145 as worthwhile for further manipulation to discover SXA variants that express improved properties over wild-type SXA for performing biomass saccharification, particularly with reference to lower affinities for D-xylose and D-glucose while maintaining good catalytic and stability properties of wild-type SXA. The approach of employing saturation mutagenesis at position 145 was obvious, but the properties of the resultant SXA mutants were not as predictable. Although, stability properties are related to hydrophobicity of the substituted amino acid side chain, $K_i^{\text{D-xylose}}$ values are not correlated well enough with stability to allow prediction of mutants that express both good stability and lower affinity for D-xylose and D-glucose such as reported here for W145F, W145L, and W145Y. The latter express modestly higher (11, 6, and 1%, respectively) k_{cat}^{X2} values than wild-type SXA, as well. The resultant 46, 71, and 48% higher rates at high (0.1 M) X2 and D-xylose concentrations, calculated for W145F, W145L, and W145Y in comparison to wild-type SXA, are valuable considering the large scale envisioned for bioreactors. It is desirable to achieve even greater improvements. Fortunately, the screen for discovery of initial leads has been designed to accommodate much larger libraries than were incorporated in this initial exercise and the positive results presented here encourage us to proceed at a larger scale.

References

1. Adelsberger H, Hertel C, Glawischnig E, Zverlov VV, Schwarz WH (2004) Enzyme system of *Clostridium stercorarium* for hydrolysis of arabinoxylan: reconstitution of the in vivo system from recombinant enzymes. Microbiology 150:2257–2266
2. Biarnés X, Nieto J, Planas A, Rovira C (2006) Substrate distortion in the Michaelis complex of bacillus 1, 3–1, 4-beta-glucanase. Insight from first principles molecular dynamics simulations. J Biol Chem 281:1432–1441
3. Brunzelle JS, Jordan DB, McCaslin DR, Olczak A, Wawrzak Z (2008) Structure of the two-subsite beta-D-xylosidase from Selenomonas ruminantium in complex with 1, 3-bis[Tris (hydroxymethyl)methylamino]propane. Arch Biochem Biophys 474:157–166
4. Cantarel BL, Coutinho PM, Rancurel C, Bernard T, Lombard V, Henrissat B (2008) The carbohydrate-active enzymes database (CAZy): an expert resource for glycogenomics. Nucleic Acids Res 37:D233–D238
5. Davies GJ, Mackenzie L, Varrot A, Dauter M, Brzozowski AM, Scülein M, Withers SG (1998) Snapshots along an enzymatic reaction coordinate: analysis of a retaining beta-glycoside hydrolase. Biochemistry 37:11707–11713
6. Durette PL, Horton D (1971) Conformational analysis of sugars and their derivatives. Adv Carbohydr Chem Biochem 26:49–125
7. Fan Z, Yuan L, Jordan DB, Wagschal K, Heng C, Braker JD (2010) Engineering lower inhibitor affinities in beta-D-xylosidase. Appl Microbiol Biotechnol 86:1099–1113
8. Fauchère J-L, Pliška V (1983) Hydrophobic parameters pi. of amino acid side chains from the partitioning of *N*-acetyl-amino acid amides. Eur J Med Chem 18:369–375
9. Gill SC, von Hippel PH (1989) Calculation of protein extinction coefficients from amino acid sequence data. Anal Biochem 182:319–326
10. Gong CS, Cao NJ, Du J, Tsao GT (1999) Ethanol production from renewable resources. Adv Biochem Eng Biotechnol 65:207–241
11. Gray KA, Zhao L, Emptage M (2006) Bioethanol. Curr Opin Chem Biol 10:141–146
12. Henrissat B (1991) A classification of glycosyl hydrolases based on amino acid sequence similarities. Biochem J 280:309–316
13. Johnson KA, Simpson ZB, Blom T (2009) Global kinetic explorer: a new computer program for dynamic simulation and fitting of kinetic data. Anal Biochem 387:20–29
14. Jordan DB, Dien BS, Li X-L, Cotta MA (2006) Hemicellulases for mediating biomass saccharification. In: Renewable Energy 2006 Committee (ed) Proceedings of renewable energy. Japan, pp 1036–1041
15. Jordan DB, Li X-L, Dunlap CA, Whitehead TR, Cotta MA (2007) Beta-D-xylosidase from *Selenomonas ruminantium* of glycoside hydrolase family 43. Appl Biochem Biotechnol 137–140:93–104
16. Jordan DB, Li X-L, Dunlap CA, Whitehead TR, Cotta MA (2007) Structure-function relationships of a catalytically efficient beta-D-xylosidase. Appl Biochem Biotechnol 141:51–76
17. Jordan DB, Li X-L (2007) Variation in relative substrate specificity of bifunctional beta-D-xylosidase/alpha-L-arabinofuranosidase by single-site mutations: roles of substrate distortion and recognition. Biochim Biophys Acta 1774:1192–1198
18. Jordan DB, Braker JD (2007) Inhibition of the two-subsite beta-D-xylosidase from *Selenomonas ruminantium* by sugars: competitive, noncompetitive, double binding, and slow binding modes. Arch Biochem Biophys 465:231–246
19. Jordan DB (2008) Beta-D-xylosidase from *Selenomonas ruminantium*: catalyzed reactions with natural and artificial substrates. Appl Biochem Biotechnol 146:137–149
20. Jordan DB, Braker JD (2009) Beta-D-xylosidase from *Selenomonas ruminantium*: thermodynamics of enzyme-catalyzed and noncatalyzed reactions. Appl Biochem Biotechnol 155:330–346
21. Jordan DB, Mertens JA, Braker JD (2009) Aminoalcohols as probes of the two-subsite active site of beta-D-xylosidase from *Selenomonas ruminantium*. Biochim Biophys Acta 1794:144–158
22. Jordan DB, Braker JD (2010) Beta-D-Xylosidase from *Selenomonas ruminantium*: role of glutamate 186 in catalysis revealed by site-directed mutagenesis, alternate substrates, and active-site inhibitor. Appl Biochem Biotechnol 161:395–410
23. Jordan DB, Wagschal K (2010) Properties and applications of microbial beta-D-xylosidases featuring the catalytically efficient enzyme from *Selenomonas ruminantium*. Appl Microbiol Biotechnol 86:1647–1658
24. Klinke HB, Thomsen AB, Ahring BK (2004) Inhibition of ethanol-producing yeast and bacteria by degradation products produced during pre-treatment of biomass. Appl Microbiol Biotechnol 66:10–26
25. Larsson AM, Bergfors T, Dultz E, Irwin DC, Roos A, Driguez H, Wilson DB, Jones TA (2005) Crystal structure of *Thermobifida*

fusca endoglucanase Cel6A in complex with substrate and inhibitor: the role of tyrosine Y73 in substrate ring distortion. Biochemistry 44:12915–12922
26. Larsson S, Palmqvist E, Hahn-Hägerdal B, Tengborg C, Stenberg K, Zacchi G, Nilvebrant NO (1999) The generation of fermentation inhibitors during dilute acid hydrolysis of softwood. Enzyme Microb Technol 24:151–159
27. Leatherbarrow RJ (2001) Grafit version 5. Erithacus Software Ltd., Horley
28. Lee YY, Iyer P, Torget RW (1999) Dilute-acid hydrolysis of lignocellulosic biomass. Adv Biochem Eng Biotechnol 65:93–115
29. Luo CD, Brink DL, Blanch HW (2002) Identification of potential fermentation inhibitors in conversion of hybrid poplar hydrolyzate to ethanol. Biomass Bioenergy 22:125–138
30. Notenboom V, Birsan C, Nitz M, Rose DR, Warren RA, Withers SG (1998) Insights into transition state stabilization of the beta-1, 4-glycosidase Cex by covalent intermediate accumulation in active site mutants. Nat Struct Mol Biol 5:812–818
31. Palmqvist E, Hahn-Hägerdal B (2000) Fermentation of lignocellulosic hydrolysates. II: inhibitors and mechanisms of inhibition. Bioresour Technol 74:25–33
32. Pattanaik S, Huan CH, Yuan L (2008) The interaction domains of the plant Myc-like bHLH transcription factors can regulate the transactivation strength. Planta 227:707–715
33. Saha BC (2003) Hemicellulose bioconversion. J Ind Microbiol Biotechnol 30:279–291
34. Sulzenbacher G, Driguez H, Henrissat B, Scülein M, Davies GJ (1996) Structure of the *Fusarium oxysporum* endoglucanase I with a nonhydrolyzable substrate analogue: substrate distortion gives rise to the preferred axial orientation for the leaving group. Biochemistry 35:15280–15287
35. Tews I, Perrakis A, Oppenheim A, Dauter Z, Wilson KS, Vorgias CE (1996) Bacterial chitobiase structure provides insight into catalytic mechanism and the basis of Tay–Sachs disease. Nat Struct Mol Biol 3:638–648
36. Vasella A, Davies GJ, Böhm M (2002) Glycosidase mechanisms. Curr Opin Chem Biol 6:619–629
37. Wagschal K, Heng C, Lee CC, Robertson GH, Orts WJ, Wong DWS (2009) Purification and characterization of a glycoside hydrolase family 43 beta-xylosidase from *Geobacillus thermoleovorans* IT-08. Appl Biochem Biotechnol 155:304–313
38. Wimley WC, Creamer TP, White SH (1996) Solvation energies of amino acid side chains and backbone in a family of host-guest pentapeptides. Biochemistry 35:5109–5124